RSC Advances

REVIEW

View Article Online
View Journal | View Issue

Cite this: *RSC Adv.*, 2026, **16**, 15913

Recent advances and challenges of analytical methods for detection of perfluoroalkyl and polyfluoroalkyl substances

Linh Q. Phan,[ab] Kien G. Nguyen [ab] and Thuan V. Tran *[ab]

Perfluoroalkyl and polyfluoroalkyl substances (PFAS) are synthetic chemicals widely used for domestic and industrial purposes. Because PFAS are highly persistent, bioaccumulative, and toxic, they pose potential threats to the environment and human health. This review provides a comprehensive overview of PFAS occurrence and monitoring across diverse environmental and biological matrices, as well as their toxicological impacts on soil microbiota, plants, animals, and humans. Advancements and limitations of PFAS analytical techniques such as liquid chromatography-mass spectrometry, gas chromatography-mass spectrometry, supercritical fluid chromatography, nuclear magnetic resonance, and high-resolution mass spectrometry are evaluated. Moreover, we explore the emerging integration of artificial intelligence and machine learning approaches in PFAS detection, classification, and toxicity prediction. These data-driven methods offer promising solutions to overcome existing analytical challenges, such as high costs, complex sample preparation, and long analysis time.

Received 22nd July 2025
Accepted 15th March 2026

DOI: 10.1039/d5ra05298j

rsc.li/rsc-advances

1. Introduction

Perfluoroalkyl and polyfluoroalkyl substances (PFAS) are synthetic chemicals widely utilized in various industrial and consumer products, such as non-stick coatings, fire-fighting foams, and water-repellent textiles.[1–3] Due to their extensive applications, PFAS have been detected in multiple environmental matrices such as water, soil, and biological systems.[4] These compounds are highly persistent, bioaccumulative, and toxic, and have been linked to severe health risks, including endocrine disruption, hepatotoxicity, and even carcinogenicity.[5–7] Because PFAS contamination is pervasive, and these compounds persist in the environment for extended periods,[8,9] effective strategies for their detection and remediation are urgently required to mitigate their environmental and health impacts.

Various analytical techniques are used to detect PFAS in biological and environmental samples, *i.e.*, gas chromatography-mass spectrometry (GC-MS), high-performance liquid chromatography (HPLC), liquid chromatography-mass spectrometry (LC-MS), nuclear magnetic resonance (NMR), high-resolution mass spectrometry (HRMS), and supercritical fluid chromatography (SFC).[10–12] While these methods exhibit high sensitivity and specificity, they typically entail costly instrumentation and complex sample preparation. Other advanced techniques, such as fluorescent detection and electrochemical sensing are currently reported to effectively detect PFAS.[13] Nevertheless, the detection of PFAS at trace levels remains a challenging task, necessitating continued refinement of analytical methods.

Numerous studies have made efforts to solve PFAS-associated problems from various viewpoints. Some have focused on quantifying PFAS concentrations in environmental compartments, such as sludge, water, wastewater, soil, and air.[14–17] Others have examined analytical trends, environmental transport, and PFAS bioaccumulation in organisms.[18–20] Additionally, various publications have been devoted to evaluating various PFAS treatment technologies and their respective advantages and limitations. These include chemical reduction, electrochemical degradation, photolysis, thermal degradation, ultrasonication, microbial degradation, and adsorption.[15,21,22] Among these approaches, adsorption has received significant attention due to its high efficiency, reusability, operational simplicity, and minimal use of toxic reagents or complex equipment.[22–30]

However, most existing reviews on PFAS adsorption primarily emphasize adsorbent types and removal mechanisms, whereas the sources of PFAS contamination and their environmental and biological impacts are rarely discussed comprehensively. For example, Gomri *et al.*,[25] Calore *et al.*,[28] and Vakili *et al.*[22] investigated adsorption mechanisms with various adsorbents, including activated carbon, biochar, ion-exchange resins, polymers, nanoparticles, zeolites, and clays. Nevertheless, these studies offer limited insights into the origins of PFAS contamination and their broader ecological and human health

[a]*Center for Hi-Tech Development, Nguyen Tat Thanh University, Saigon Hi-Tech Park, Ho Chi Minh City, Vietnam. E-mail: tranvt@ntt.edu.vn; Tel: (+84) 0902 298 300*
[b]*Institute of Applied Technology and Sustainable Development, Nguyen Tat Thanh University, Ho Chi Minh City, Vietnam*

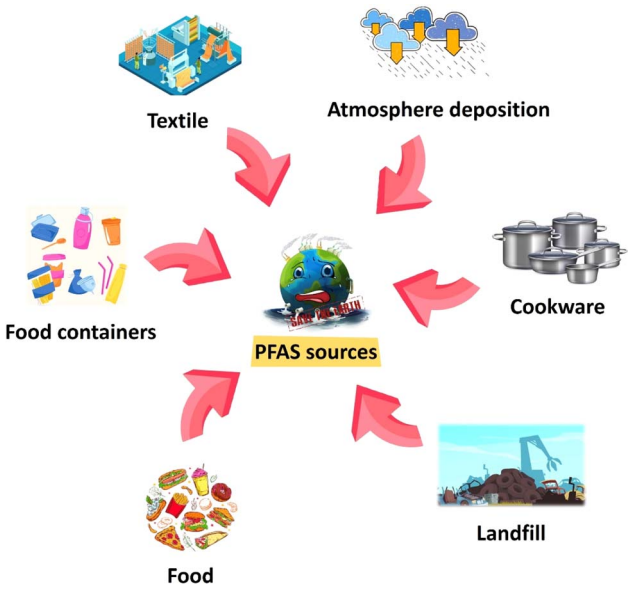

Fig. 1 The original source of PFAS in the environment.

implications. Therefore, this review aims to bridge this gap by providing a comprehensive overview of PFAS occurrence in the environment, their effects on living organisms, and their removal through adsorption using various adsorbent materials (Fig. 1).

2. Occurrence of PFAS in various environmental and biological matrices

2.1. Global distribution and pathways of PFAS contamination

2.1.1. PFAS in drinking water and groundwater sources. The presence of PFAS in drinking, surface water, and groundwater sources has been observed worldwide at varying concentrations and compound types (Table S1). A comprehensive survey of five aquifer systems from 254 wells in the USA detected 24 types of PFAS at concentrations of 1–1000 ng L^{-1}.[31] Notably, more than 80% of the detected PFAS consisted of PFOA, PFOS, and PFBS. Additionally, PFAS with carbon chain lengths between four and nine exhibited significantly higher detection frequencies, from nearly 10% to nearly 50% compared to other compounds.

In China, surface and groundwater samples collected near fluorochemical industrial zones revealed the predominance of short-chain PFAS, including PFOA, perfluorobutanoic acid (PFBA), and PFBS, but at comparatively higher concentrations.[32] PFAS levels in surface and groundwater ranged from were 0.4–765 μg L^{-1} and 0.6–306 μg L^{-1}, respectively. In most industrial zones, the PFAS compounds containing four to eight carbon atoms were dominant. The authors attributed this trend to national regulatory frameworks that still permit the use of certain PFAS and the lack of unified international emission limits for PFOA.[32] Another reason was suggested that the short-chain PFAS (*e.g.*, PFBA, PFBS) are more water-soluble than long-chain PFAS. This allows them to disperse easily in water bodies, groundwater, and drinking water sources.

Widespread PFAS contamination has also been documented in rivers in Spain and Colombia, where short-chain compounds are frequently dominant. In the Besòs River Delta in Spain, 19 types of PFAS, belonging to TFA, TFSA, PFAAs, PFBA, PFPeA, PFHxA, and PFBS, were detected at very high concentrations, from 109 ng L^{-1} to 1007 ng L^{-1}.[33] Similarly, the PFAS contamination in Bogotá River in Colombia also revealed the existence of PFPeA in five of six samples analyzed.[34] However, downstream water samples exhibited higher levels of long-chain PFHxS (520 ng L^{-1}) and PFOS (240 ng L^{-1}). The authors attributed these elevated levels to the influence from nearby industrial activities, such as tanneries, mining operations, food production, and petrochemical industries, as well as wastewater and industrial waste plants, combined with the geographical characteristics of these regions.

2.1.2. PFAS accumulation in food products and household materials. The accumulation of PFAS in food products and household materials have been documented with the prevalence of PFOS, PFOA, and FTOH containing six to ten carbon atoms (Table S1). For example, Huang *et al.*[35] evaluated the contamination of PFAS in fast foods, *e.g.*, ice cream, instant noodles, and bubble tea. They found that 27 kinds of PFAS with the concentration ranged from below the limit of detection to 2.1 ng g^{-1}. In these fast foods, the long-chain compounds, *e.g.*, 6 : 2 diPAP, 6 : 2 PAP, and PFOA accounted for the majority of proportion of PFAS, whereas short-chain PFAS were less abundant. The authors presumed that long-chain PFAS are more lipophilic as indicated by the high oil-water partition coefficient (log *P*), whereas short-chain PFAS with lower log *P* values, are more water-soluble. PFAS contamination in fast foods primarily arises during manufacturing, storage, and packaging processes. Therefore, ice cream, instant noodles, and bubble tea retains long-chain PFAS, leading to greater accumulation.

Similarly, a study conducted in Antwerp, Belgium, reported frequent detection of PFOA and PFOS in eggs.[36] Among detected 17 PFAS compounds, the concentrations of PFBA and PFOS were the highest at 9.1 ng g^{-1} and 214 ng g^{-1}, respectively. The authors presumed that despite PFOS and PFOA have been gradually phased out in Europe since 2002, PFOS residuals in soil remains extremely persistent due to its strong adsorption to soil particles. This property allows PFOS to remain in subsurface layers for extended periods, resulting in long-term environmental persistence and potential uptake by hens, thereby transferring PFAS into eggs.

In paper-based food packaging, long-chain PFAS were found in significantly higher amounts than short-chain PFAS. Vázquez Loureiro *et al.*[37] reported that paper-based muffin cups contained 13 types of PFAS, with a predominance of long-chain compounds such as 6 : 2 to 10 : 2 FTOH, PFOA, PFDA, PFUnDA, and PFDoDa. Notably, FTOH compounds (*e.g.*, 6 : 2, 8 : 2, and 10 : 2 moieties) accounted for approximately 90% of the total PFAS content, with the highest concentration up to 11.5 μg kg^{-1}. In contrast, short-chain PFAS (PFPeA, PFHpA, and PFHxA) represented less than 3% of total PFAS, with concentrations of 0.028 μg kg^{-1}, 0.041 μg kg^{-1}, and 0.16 μg kg^{-1},

respectively. This distribution pattern likely results from the widespread use of FTOHs in grease-resistant coatings for food packaging and their high environmental persistence. Moreover, since FTOHs act as precursors to PFOA, the transformation process occurs gradually, explaining the relatively low PFOA concentration (3% of total PFAS, equivalent to 0.38 μg kg^{-1}) detected in the muffin cup samples.

2.2. Biomonitoring and human exposure

2.2.1. PFAS levels in human body. Biomonitoring studies have revealed the widespread presence of PFAS in human blood serum, exhibiting a broad range of compound types and concentrations (Table S1, please see in the SI file). In a survey of 605 adults in the United States, 38 PFAS species were detected in serum blood samples at concentrations ranging from below detection limits to 32.9 ng mL^{-1}.[38] Noticeably, long-chain PFAS (*e.g.*, PFOS, PFOA, PFNA, PFHxS, PFDA, and PFHpS) were detected in 96% of participants. Meanwhile, most short-chain PFAS (C4–C6 compounds, including PFBS, PFBA, PFPeA, and PFHxA) showed much lower detection frequencies from 0.3% to 28.6%. Age-related trends were also observed, with older adults (aged 60 years and above) exhibiting higher PFAS levels than younger individuals, suggesting bioaccumulation with age.

Similarly, Suzuki *et al.*[39] analyzed PFAS concentrations in blood serum collected from deceased individuals and detected 20 PFAS compounds. Among these PFAS, long-chain compounds, such as PFOS, PFDA, PFUnDA, PFOA, and PFNA were present in all serum bloods with concentrations from 0.04 ng mL^{-1} to 13 ng mL^{-1}, higher than those of short-chain PFAS. Other studies also confirmed that long-chain PFAS possess a higher bioaccumulation potential due to their strong affinity for binding to serum proteins and their tendency to accumulate in the liver and other tissues over time.[40,41]

More investigations into PFAS accumulation in the human brain and cerebrospinal fluid (CSF) further support the predominance of long-chain compounds. Suzuki *et al.*[39] detected PFAS in the temporal pole and middle frontal cortex of deceased individuals with detection frequencies of approximately 80% for both short-chain PFHxS and long-chain, *e.g.*, PFNA, PFOS, PFDA, PFUnDA, and N-MeFOSAA. The concentration of PFHxS in both brain region samples only ranged from 0.05 to 0.97 ng g^{-1}, while long-chain PFAS were detected at 0.02–2.7 ng g^{-1}. In another study, Hu *et al.*[42] observed that in cerebrospinal fluid of human, 26 target PFASs were found with the quantities from below the limit of detection to 11.8 ng mL^{-1}. The proportion of these long-chain, *e.g.*, 6 : 2 FTSA, PFOS, and PFOA accounted for more than 75% PFAS compounds with the average concentration at 0.26 ng mL^{-1}, 0.22 ng mL^{-1}, and 0.12 ng mL^{-1}, respectively. The authors proposed three key factors explaining the predominance of long-chain PFAS in human tissues. First, these compounds are widely used in consumer products and remain prevalent in the surrounding environment. Second, their hydrophobic nature enables interaction with brain tissue phospholipids, facilitating passage across the blood–brain barrier. Third, long-chain PFAS exhibit high bioaccumulation potential and resistance to degradation in both biological and physical media, resulting in their persistence within the human body.

Along with their presence of PFAS in human blood and organs, PFAS have also been detected in human breast milk, though generally at lower concentrations. A survey conducted in Washington, USA, reported 39 PFAS compounds in breast milk samples, with concentrations ranging from 52 to 1850 pg mL^{-1}.[43] Among them, long-chain PFAS, *e.g.*, PFOA and PFOS, exhibited the highest mean concentrations from 15 to 30 pg mL^{-1}, while short-chain PFAS, including PFHpA and PFHxA were detected at 6–10 pg mL^{-1}. Similarly, Blomberg *et al.*[44] analyzed breast milk samples from women in Ronneby, Sweden, and detected both long- and short-chain PFAS. The findings showed a comparable pattern with PFOS and PFOA being the predominant long-chain PFAS, occurring at concentrations of 40–390 and 20–60 pg mL^{-1}, respectively. Among the short-chain PFAS, PFHxS was detected in 75% of the measured samples and at concentrations 10–320 pg mL^{-1}.

2.2.2. Role of diet in PFAS exposure. Diet plays a crucial role in PFAS exposure across different sociodemographic groups, influencing the levels and types of PFAS detected in humans. Among sensitive groups such as pregnant women and newborns, dietary intake significantly affects PFAS concentrations. Fábelová *et al.*[45] examined the PFAS levels in maternal blood and cord blood from 6837 participants in 19 European cohorts. They found that the PFAS quantities in maternal blood of pregnancy women were larger, *e.g.*, PFOS (10.9 μg L^{-1}), PFOA (2.3 μg L^{-1}), PFHxS (0.6 μg L^{-1}), and PFNA (0.5 μg L^{-1}) than those in newborns at 0.99, 1.27, 0.15, and 0.22 μg L^{-1}, respectively. The statistical results revealed that greater PFAS concentrations in maternal blood were associated with increased consumption of seafood, meat, offal, and eggs. In contrast, PFAS levels were comparatively lower; however, elevated PFHxS and PFNA concentrations were linked to high daily consumptions of meat and offal. This relationship likely arises because animals living in PFAS-contaminated environments accumulate PFAS from their surroundings and diets, which subsequently leads to biomagnification through the food chain.

Similarly, a past study of 2545 pregnant women from the Shanghai Birth Cohort reported that animal-based foods were significant contributors to PFAS accumulation.[46] The findings reported that concentrations of 10 PFAS compounds ranged from 0.02 to 14.8 ng mL^{-1}. High concentrations of PFOA, PFOS, PFBS and PFHxS were positively correlated with the consumption of seafood (*e.g.*, shrimp and crab) and animal organs (*e.g.*, kidneys, liver, and bones). Notably, the majority of pregnant women who consumed plant-based foods, *i.e.*, vegetables, fruits, beans, and fiber-rich foods at a moderate or higher frequency had significantly lower concentrations of PFNA, PFDA, and PFUA.

Dietary fiber and plant-based foods also appear to mitigate PFAS accumulation in other populations. Indeed, Hampson *et al.*[47] reported that the consumption of whole fruits, cooked grains (*e.g.*, rice and oatmeal), grain-based foods (*e.g.*, bread and pasta), and vegetables in Hispanic young adults in Southern California resulted in low exposure to PFAS. As fruits,

vegetables, and grains are major sources of dietary fiber, these findings suggest that higher fiber intake may promote PFAS elimination and help lower body burdens.

Furthermore, dairy consumption also showed an inverse correlation with the concentration of PFAS in human serum. Fábelová *et al.*[45] and Sultan *et al.*[48] reported that dairy-rich diets, particularly those including milk, were not associated with elevated PFAS levels in newborns, women, or adolescents. Dairy intake may enhance intestinal motility and improve digestive efficiency, thereby facilitating PFAS excretion through feces rather than accumulation in blood. Interestingly, lactose-intolerant individuals may experience even faster PFAS elimination. However, Vestergren *et al.*[49] measured that approximately 39% of the total PFAS in cows was eventually excreted into milk, suggesting potential exposure through dairy products, albeit at lower levels.

Recently, Zhou *et al.*[50] revealed that pro-inflammatory diets (*e.g.*, ultra-processed foods, refined carbohydrates, unhealthy fats, and added sugars) can exacerbate PFAS-induced oxidative stress and inflammation. Their study identified a novel interaction, that is, individuals with high dietary inflammatory index scores exhibited stronger associations between PFAS exposure and biomarkers, *e.g.*, neutrophil count and alkaline phosphatase, which indicated synergistic adverse effects. Notably, anti-inflammatory nutrients such as dietary fiber and vitamin D correlate with reduced PFAS concentrations. Interestingly, while n-3 polyunsaturated fatty acids are typically regarded as beneficial, they were found to correlate with elevated PFAS levels. This leads to the complex and context-dependent nature of dietary influences on PFAS exposure.

2.2.3. Role of occupation in PFAS exposure. Apart from diet, occupational exposure to PFAS is a main factor that often result in serum concentrations higher than those found in the general population group.[51] At the workplace, fluorochemical workers exposure to PFAS through inhalation of aerosolized particles and dermal absorption from handled materials. Indeed, Freberg *et al.*[52] indicated that professional ski waxing technicians exposed to very high levels of fluorinated vapors and dust during the thermal application of waxes. PFOA was detected in serum at the highest median concentration of 50 ng mL^{-1}, approximately 25 times higher than the general population. Moreover, this cohort provided the first evidence for perfluorotetradecanoic acid in human serum.

Firefighting remains another high-risk occupation in comparison to other occupations due to the use of aqueous film-forming foam and the presence of PFAS in personal protective equipment.[53,54] Mitchell *et al.*[55] revealed that firefighters had the highest concentrations of PFHxS and PFOS compared to other essential workers, including healthcare staff. Similarly, Trowbridge *et al.*[56] also confirmed that female firefighters in San Francisco found significantly higher levels of PFHxS, PFUnDA, and PFNA compared to female office workers. Hence, even within the same geographic region, occupational tasks create a distinct "toxicological fingerprint".

2.2.4. Role of lifestyle in PFAS exposure. Dietary habits represent one of the most significant non-occupational pathways for PFAS bioaccumulation mainly due to the consumption of specific food groups acting as a primary driver of serum concentration variability. Biomonitoring programs in Michigan, Minnesota, New York and Wisconsin identified a strong correlation between the consumption of locally caught fish and significantly elevated levels of PFAS.[57,58] Yamada *et al.*[59] found that frequent seafood consumers were the dietary population that most exposed to PFOA, PFNA, and PFHxS.

2.3. PFAS in wildlife and agriculture systems

2.3.1. Influence of PFAS on soil microbiota and plant uptake. The impact of PFAS on plant uptake varies among species and plant tissues, reflecting differences in accumulation and translocation behavior. Nassazzi *et al.*[60] investigated the concentration of PFAS on *Helianthus annuus*, *Brassica juncea*, and *Cannabis sativa* and observed that 12 types of PFAS were detected in different tissues, with each PFAS administered at a concentration of 1.5 mg kg^{-1}. Among these species, *Brassica juncea* exhibited the highest accumulation capacity with PFAS concentrations two to seven times greater than those in *Helianthus annuus* and *Cannabis sativa*. In the seeds, stems, and leaves of all three plants, short-chain PFAS were frequently detected (60–90%) at concentrations from 29 ng g^{-1} to 21 669 ng g^{-1}. Meanwhile, long-chain PFAS, *e.g.*, PFSA and PFCAs predominated in roots with detection frequencies between 27% and 52% and concentrations from 3.3 ng g^{-1} to 10 551 ng g^{-1}. The authors explained that because short-chain PFAS are more water-soluble and mobile, they are likely to be translocated through water uptake and transpiration to aerial parts of the plants.[61] In contrast, long-chain PFAS tend to remain in roots due to their hydrophobicity, persistence, and higher bioaccumulation potential.

Jiang *et al.*[62] also reported consistent results in soybean roots, where long-chain PFAS were detected more frequently than short-chain compounds. Using the translocation factor (TF) index calculated as the ratio of PFAS concentrations in stems and roots, the authors found that long-chain PFAS exhibited lower TF values (0.09–0.19) than short-chain PFAS (1–16). This difference was attributed to the greater hydrophilicity of short-chain PFAS, which facilitates their migration through the xylem along with water and mineral ions. Interestingly, soybean plants exposed to a PFAS mixture showed significantly higher PFOA and PFOS concentrations than those exposed to individual compounds at equivalent levels. This suggests that the synergistic effects of PFAS mixtures enhance the uptake of individual PFAS.

PFAS contamination also exerts pronounced effects on soil microbiota. Liu *et al.*[63] showed that PFAS exposure markedly reduced rhizosphere microbial diversity. In the control sample (without PFAS), 308 microbial species were identified, while PFAS-contaminated soils contained only 32–108 species. Such reductions indicate that PFAS disturb rhizosphere microbial community structure, disrupting ecological balance and potentially impairing soil and plant health. These changes may also propagate through the food chain, indirectly affecting animals and humans.

Recently, Jiang *et al.*[62] analyzed genetic changes in the microbial communities of PFAS-exposed soybean soils. These researchers observed that PFAS substantially altered nitrogen-

cycling gene abundance in both bulk and rhizosphere soils. PFAS exposure suppressed nitrification genes (*AOA* and *AOB amoA*) and denitrification genes, while mixtures of PFAS upregulated the nitrogen-fixation gene *nifH* in soybean nodules. These findings suggest that PFAS disrupt key soil microbial processes, particularly those involved in nitrogen cycling. Therefore, monitoring and regulating PFAS concentrations in soil are essential for preserving microbial community stability and supporting the sustainable development of terrestrial ecosystems.

2.3.2. Contamination of PFAS in domestic animals and wildlife. PFAS contamination has also been documented in domestic animals with measurable levels detected in all horse and dog blood samples analyzed.[64] Overall, PFAS concentrations were higher in dogs than in horses, averaging at 0.0029 mg L^{-1} and 0.0018 mg L^{-1}, respectively. This disparity likely reflects dogs' greater exposure to indoor sources such as drinking water and household dust. Notably, dogs consuming well water exhibited significantly higher PFOS (0.00493 mg L^{-1}) and PFHxS (0.00326 mg L^{-1}) levels in their blood compared to those drinking bottled water (PFOS: 0.00174 mg L^{-1}, PFHxS: 0.00054 mg L^{-1}). PFAS exposure was also linked to alterations in health biomarkers. Indeed, dogs showed elevated alkaline phosphatase and alanine aminotransferase levels, while horses exhibited higher creatine kinase and gamma-glutamyl transferase levels, indicating potential kidney and liver stress. These fluctuations in biochemical markers suggest that PFAS exposure can adversely affect internal organ function. Therefore, minimizing PFAS contamination in the environment is essential for safeguarding the long-term health of domestic animals, alongside conventional veterinary care and nutrition.

Several studies also investigated PFAS bioaccumulation across a range of wildlife species. For example, seventeen types of PFAS contamination were detected in various vertebrates at Holloman Air Force Base with concentrations from 0.024 mg kg^{-1} to 97 mg kg^{-1}.[65] Fig. 2 shows heat map on the PFAS concentration across different clades, tissues, and species. Aquatic birds and littoral-zone house mice exhibited the highest PFAS levels with PFOS averaging greater than 10 mg kg^{-1}, while upland desert rodents showed significantly lower concentrations. These variations can be attributed to differences in exposure pathways. Aquatic organisms ingest PFAS through contaminated water, sediments, and prey, while terrestrial rodents experience less direct contact. PFHxS concentrations were also elevated in littoral mice and aquatic birds, up to 11 mg kg^{-1}, whereas upland rodents accumulated PFAS to a much lesser extent.

In another study, PFAS exposure in birds and mammals from the marine and terrestrial Norwegian was also investigated.[66] The analysis revealed 73 types of PFAS found in the eggs in birds and in plasma and liver samples of mammals. Total PFAS concentration ranged from 0.006 mg kg^{-1} to 0.045 mg kg^{-1} in birds and from 0.00074 mg kg^{-1} to 0.27 mg kg^{-1} in mammals. Notably, long-chain PFCAs, *e.g.*, PFUnDA and PFTrDA constituted more than half of the total PFAS burden in seabirds. Meanwhile, PFNA, PFDA, and PFUnDA collectively accounted for over 70% of the PFAS in most mammalian samples. In mammalian samples, PFNA, PFDA, and PFUnDA together accounted for over 70% of the total PFAS content. The authors attributed these discrepancies to differences in species-specific feeding behaviors, habitats, and regional contamination sources, particularly among marine mammals.

2.3.3. PFAS transfer through biosolids and irrigation practices. PFAS transferring through biosolids is one of the most common modes of PFAS contamination. Levine *et al.*[67] evaluated PFAS leaching from different compost amendments and reported distinct differences in leaching potential among PFAS types. Short-chain PFAS, such as PFHxA and PFBS, exhibited higher leaching capacities with concentrations ranging from 0.31 to 1.2 μg L^{-1}. PFHxA was detected in 7.8% of all samples but declined below detection limits after four weeks, while PFBS was found in 20% of samples without a consistent temporal pattern. In contrast, long-chain PFAS, *i.e.*, PFOA, remained persistently elevated throughout the study, occurring in 33% of samples with a mean concentration of 0.14 μg L^{-1}. The authors interpreted that greater mobility of short-chain PFAS led to rapid leaching of total PFAS. On the other hand, long-chain PFAS exhibit strong sorption to soil particles, giving rise to their long-term persistence. While PFAS were detected in compost leachates, levels were below regulatory limits and presented minimal risk to the ecosystem. However, long-term groundwater contamination and bioaccumulation potential still need to be assessed by continued monitoring.

Irrigation water has also been identified as a significant source of PFAS exposure, as demonstrated by hydroponic cultivation studies. Gu *et al.*[68] investigated PFAS accumulation in lettuce, cabbage, and cucumber exposed to 17 PFASs with concentrations in plants from 4.000 μg g^{-1} to 13.456 μg g^{-1}. The study revealed a U-shaped relationship between PFAS accumulation and the root concentration factor (RCF), defined as the ratio of PFAS concentration in plant roots to that in the hydroponic solution. For instance, the RCF of PFBA in lettuce reached 98, decreased to 26 for PFHxA, and increased sharply to 2437 for PFUnDA. This pattern reflects a negative correlation between PFAS chain length and root absorption. Short-chain PFAS (*e.g.*, PFBA, PFHxA) were more readily absorbed due to their higher hydrophilicity. Meanwhile, long-chain PFAS (*e.g.*, PFUnDA) showed stronger adsorption on root surfaces owing to their hydrophobicity and larger molecular size.

Similarly, another study on PFAS bioaccumulation in hydroponically grown lettuce confirmed this distinction.[69] Under an exposure concentration of 5 μg L^{-1} in the hydroponic medium, long-chain PFCAs and PFUnDA accumulated in lettuce roots at concentrations from 109 ng g^{-1} to 348 ng g^{-1}. Meanwhile, short-chain PFAS were detected at much lower levels (1.8–20 ng g^{-1}). This difference arises because both root surface adsorption and internal uptake govern PFAS accumulation. Long-chain PFAS tend to adhere to the lipophilic root surface and bind strongly to root cell membrane proteins rather than being translocated into internal tissues.[70,71]

3. Toxicology of PFAS

3.1. Impact on liver, kidneys, and immune system

Exposure to PFAS has been linked to impaired functioning of vital human organs, including the liver, kidneys, muscles, and

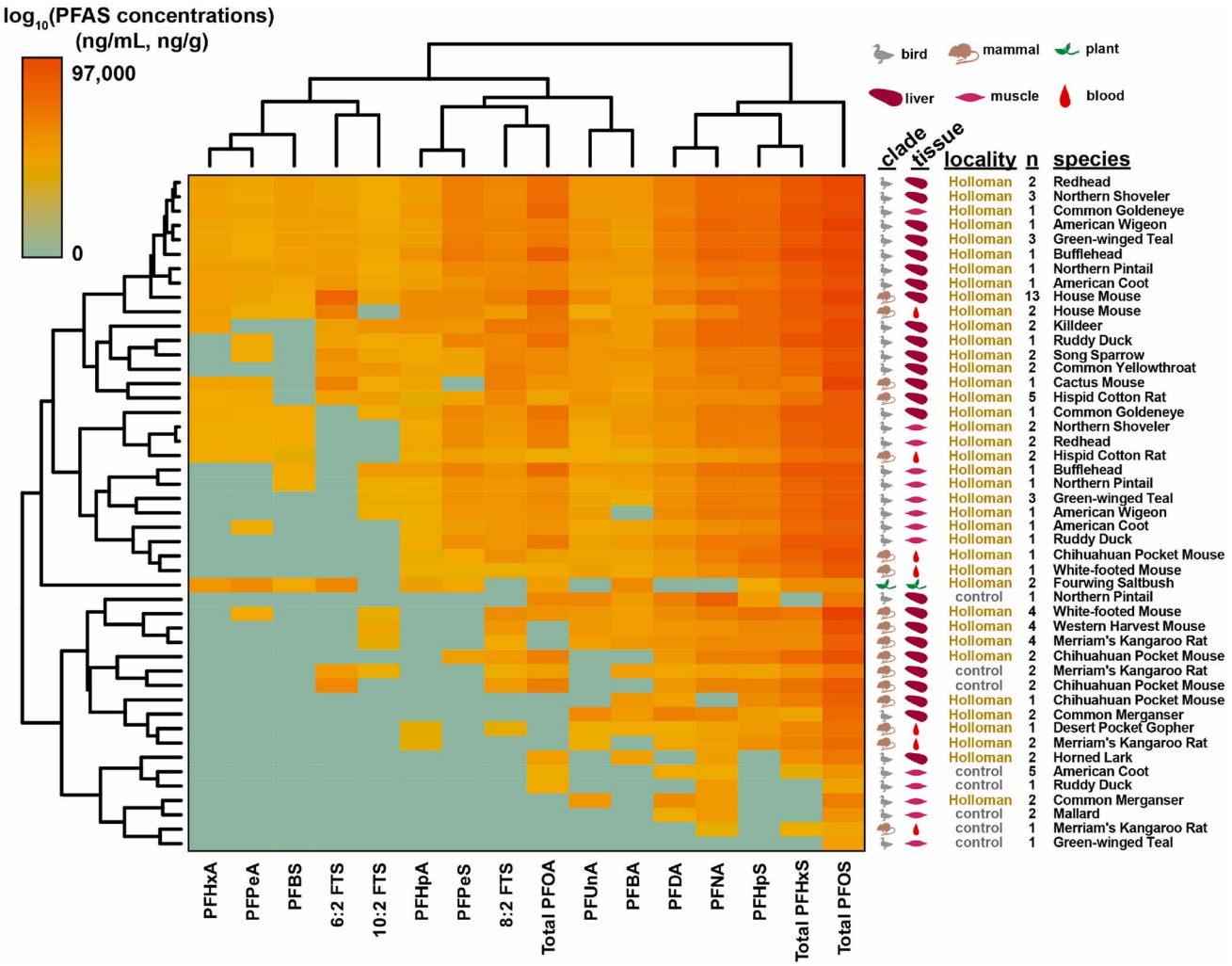

Fig. 2 Heat map showing the PFAS concentration across different clades, tissues, and species. Reprinted with the permission from ref. 65 Copyright (2024), Elsevier.

microglia. For instance, Niu *et al.*[72] proved that PFAS exposure significantly increases uric acid levels and the risk of hyperuricemia in human. Each log-unit increase in PFAS was associated with 4.2–11.6 μmol L^{-1} rise in uric acid levels, while the risk of hyperuricemia increased by 6–28%. Noticeably, the decline in kidney function mediates the PFAS-induced elevation of uric acid and the risk of hyperuricemia. Each log-unit increase in PFAS corresponded to a decline in the estimated glomerular filtration rate from −2.06 mL min^{-1} per 1.73 m^2 to −3.22 mL min^{-1} per 1.73 m^2. The authors concluded that there is no safe threshold of PFAS exposure; as even low concentrations may have adverse health effects. Moreover, they identified reduced kidney function as a key mechanism contributing to hyperuricemia following PFAS exposure.

Similarly, Solan *et al.*[73] reported that PFAS exposure induces intracellular reactive oxygen species (ROS) generation in liver cells, leading to oxidative stress in kidney, muscle, and microglia cell lines. At a PFAS concentration of 1 μM, ROS production in liver cell lines was 5.8 times higher than in control groups. Under the same exposure conditions, the activities of antioxidant enzymes, such as glutathione peroxidase, catalase, and superoxide dismutase increased by 2.3 to 7.4 times compared to controls. However, excessive upregulation of these enzymes is not necessarily beneficial, as the overproduction of ROS can lead to cellular oxidative damage and metabolic dysfunction.

In addition to hepatic and renal effects, PFAS exposure has been conclusively associated with immune-mediated disorders across various age groups, including infants, adolescents, and adults. Recent studies have linked PFAS in breast milk to a reduction in the efficacy of secretory immunoglobulin antibodies.[74] Due to the strong binding affinity of PFAS to secretory immunoglobulins, these interactions may disrupt immune protein function and increase health risks for infants. Similarly, a survey among U.S. adolescents revealed that moderate to high serum levels of PFHxS, PFOA, and PFNA (0.7–5.1 ng mL^{-1}) were associated with asthma, wheezing, and immunosuppression.[75] In adults from in the Czech Republic, another study identified PFOA, PFOS, and PFUnDA as significant contributors to atopic eczema and allergic diseases.[76] Thus, chronic PFAS exposure

may impair immune regulation, heightening susceptibility to allergic and autoimmune disorders.

In terms of mechanistic insights, the toxicology of PFAS compounds can be due to their structural role as fatty acid mimetics.[77] Indeed, C–F bonds of PFAS are highly stable and biologically persistent. Such property allows them to interact with nuclear receptors, *e.g.*, peroxisome proliferator-activated receptor alpha (PPARα).[78] When PFAS compounds bind to PPARα, they cause the conformational change of PPARα. This promotes the expression of genes involved in lipid metabolism and peroxisome proliferation.[79] However, PFAS can interact through non-PPARα pathways, including the indirect activation of the constitutive androstane receptor, and the pregane X receptor.[80] The indirect activation mechanism involves dephosphorylation that is PPARα-independent. These interactions lead to mitochondrial dysfunction and the induction of oxidative stress. Furthermore, PFAS exposure exhibits potent immune modulation by disrupting signaling in B-lymphocytes (B cells) and altering cytokine production (*e.g.*, IL-6 and TNF-α).[81] This immunotoxicity is a critical driver for the low regulatory limits recently proposed, as it directly correlates with suppressed immune responses and decreased vaccine efficacy in pediatric populations.

3.2. Neurotoxicity and endocrine disruption

Neurotoxicity induced by PFAS exposure has been widely documented in recent years. Ríos-Bonilla *et al.*[82] investigated the neurite outgrowth inhibition by PFAS mixtures, and indicated that 12 tested PFAS compounds inhibited neurite outgrowth in differentiated SH-SY5Y neuroblastoma cells. Among them, PFOS, PFOA, and PFNA exhibited the strongest inhibitory effects, reducing neurite outgrowth by 27%, 21%, and 17%, respectively. The authors claimed that PFOS, PFOA, and PFNA have higher liposome-water distribution ratios (3.5–4.9); therefore, they easily accumulate in biological membranes, thereby increasing cellular toxicity and impairing neurite outgrowth.

PFOS, one of the most persistent and abundant PFAS compounds, can also act synergistically with other environmental contaminants. For example, PFOS in combination with glyphosate (a common herbicide ingredient) to induce neuroinflammatory responses in SH-SY5Y neuronal and C6 astrocytic cell lines.[83] This synergistic toxicity was observed at an IC_{50} value of 4.59 μM after 48 h of exposure, compared to individual IC_{50} value of 68.14 μM for glyphosate and 11.43 μM for PFOS. Furthermore, PFAS exposure in offspring has been linked to neurobehavioral and developmental impairments. The total of PFAS concentrations in serum was 8–1307 ng mL^{-1}.[84] First, offspring exposed to PFAS displayed delayed acquisition of the negative geotaxis reflex, slower motor development. Second, male offspring in the exposure group had lower weights compared to low exposure groups. These findings suggest that PFAS exposure can interfere with normal neurodevelopment and affect motor coordination and sex-specific behavioral patterns. Consequently, the long-term neurodevelopmental consequences of PFAS exposure warrant comprehensive investigation.

In addition to neurotoxicity, numerous studies have identified PFAS as endocrine-disrupting chemicals capable of interfering with sex hormone production and pubertal development. He *et al.*[85] revealed in a survey of PFAS-exposed 921 adolescents in the USA that PFAS exposure was associated with decreased total testosterone levels, elevated sex hormone-binding globulin (SHBG) levels, and reduced estradiol concentrations in pubertal individuals. Zhang *et al.*[86] explained that PFAS may competitively bind to sex hormone binding globulin, inhibit steroidogenic enzyme activity, and interfere with sex hormone biosynthesis, thereby disturbing endocrine balance. Similarly, Averina *et al.*[87] found that PFAS exposure significantly impacted puberty development scores in boys and early menarche in girls. Specifically, PFDA and PFUnDA were positively associated with early menarche, while PFAS and PFOA were positively associated with puberty development score in boys. In girls, PFOA considerably altered the free testosterone index. By contrast, PFOA and PFHpA strongly affected to androstendione and 17-OH-progesterone and estradiol in boys. Thus, the significant impact of several PFAS on hormonal imbalance and precocious pubert in adolescents requires careful monitoring by health authorities to assess potential risks and implement preventive measures.

3.3. Reproductive and fetal development concerns

Human reproductive health is negatively affected by PFAS exposure. To evaluate the impact of PFAS on fertility, Zhan *et al.*[88] compared groups of women with and without experiencing polycystic ovarian syndrome. The outcome revealed that PFAS mixture in plasma was linked to an increased prevalence of polycystic ovarian syndrome. Notably, PFAS compounds such as Cl-PFESA and HFPO-DA 6 : 2 exhibited the highest percentage of 29% and 39% of the common group for polycystic ovarian syndrome, respectively. Several studies elucidated that 6 : 2 Cl-PFESA and HFPO-DA may disrupt the expression of key hormones and receptors involved in hypothalamic–pituitary–ovarian axis signaling, potentially increasing the risk of polycystic ovarian syndrome under PFAS exposure.[89,90] In another study, the occurrence of 13 types of PFAS in placenta tissue of 50 Israeli women was associated with the series of pregnancy-related complications.[91] Specifically, 70% of participants experienced gestational diabetes mellitus, while 20% developed preeclampsia. In these cases, PFOA concentrations in placental tissue were detected with the highest value (0.09 ng g^{-1}) compared to other PFAS (0.02–0.06 ng g^{-1}). Both individual PFOA exposure and PFAS mixtures are linked to insulin resistance, disruption of glucose metabolism, and the onset of preeclampsia through mechanisms involving vascular damage and oxidative stress.[92–95]

Along with reproductive complications, PFAS exposure also poses serious risks to fetal development. Zhang *et al.*[96] observed that prenatal PFAS exposure was associated with lower birth weight and reduced gestational age. Among six PFAS detected in the plasma of pregnant women during early gestation, PFOA

exposure corresponded to an average reduction of 89.1 g in birth weight. Meanwhile, PFNA exposure was associated with a 2.3 day decrease in gestational age. These effects were particularly pronounced in mothers with the lowest plasma folate levels. The authors suggested that PFAS may interfere with placental nutrient transport by competing for membrane transporters and may also induce epigenetic modifications such as DNA methylation in cord blood. Similarly, Groisman *et al.*[91] also mentioned that 10% of the surveyed population had small-for-gestational-age infants. PFAS exposure has a pronounced impact on fetal development, lowering birth weight and gestational age.

PFAS contamination not only impacts natural conception and pregnancy outcomes but also impairs success rates in assisted reproductive technologies such as *in vitro* fertilization (IVF). Shen *et al.*[97] detected eight PFAS compounds in the plasma of Chinese women undergoing IVF treatment. PFNA exposure was linked to reduced numbers of retrieved oocytes (<1.3), two PN zygotes (<0.9), and cleavage embryos (<0.8) among women in the highest PFNA quartile (2.34–32.19 ng mL^{-1}) compared to those in the lowest quartile (0.18–1.13 ng mL^{-1}). Additionally, PFOS led to the decrease of 2 PN zygotes (<0.7) and cleavage embryos (<0.5). PFHxS was found to negatively affect clinical pregnancy rates in frozen embryo transfer cycles. Mechanistically, these effects are liked to PFAS-induced interference with peroxisome proliferator-activated receptor signaling, oxidative stress, and apoptosis pathways, ultimately impairing oocyte maturation. The findings suggest that PFAS exposure can increase female infertility risk by disrupting ovarian function and steroid hormone synthesis.

4. Advancements in the detection of PFAS

4.1. Evolution of PFAS analytical techniques

4.1.1. Liquid chromatography-mass spectrometry. Liquid chromatography-mass spectrometry (LC-MS) is the most prevalent analytical technique for PFAS detection due to high selectivity and sensitivity.[98] This method allows for precise differentiation and quantification of PFAS at trace concentrations in complex environmental and biological matrices. LC-MS provides robust quantitative accuracy, making it suitable for use in regulatory monitoring and environmental risk assessment.[99]

Recently, Zou *et al.*[98] developed an advanced LC-MS method integrating large-volume injection with online solid-phase extraction for simultaneous detection and quantification of ultrashort-chain, short-chain, and long-chain FPAS. With matrix effects ranging from 80% to 120%, the method obtained high analytical reliability and was validated for diverse water samples, including surface water, sewage effluent, and seawater (Fig. 3). Similarly, LC-MS can effectively analyze both long- and short-chain PFAS without requiring derivatization. For example, Taniyasu *et al.*[100] successfully quantified perfluorinated acids in rainwater samples at sub-ng L^{-1} concentrations using a high-performance liquid chromatography-tandem mass spectrometry.

However, LC-MS remains a costly technique, requiring sophisticated instrumentation and highly trained personnel for operation and data interpretation. This method is also prone to ion suppression, particularly in complex matrices such as salts and biosolids, which can compromise analytical accuracy.[101] Despite these limitations, LC-MS continues to be regarded as the gold standard for PFAS detection across various environmental and biological media. Recent advancements have integrated ion mobility spectrometry and quadrupole time-of-flight mass spectrometry (QTOF-MS) within LC systems, achieving higher analytical precision and shorter analysis times.[102] These hybrid systems enhance target identification by incorporating collision cross-section values, thereby improving confidence in compound characterization and quantification.

4.1.2. Gas chromatography-mass spectrometry. Gas chromatography-mass spectrometry (GC-MS) is another analytical technique employed for detecting volatile or derivatized PFAS. Compared to LC-MS, GC-MS requires chemical derivatization to render PFAS molecules volatile and suitable for chromatographic separation.[103] This method is highly effective for analyzing volatile and semi-volatile PFAS, such as fluorotelomer alcohols and perfluorooctane sulfonamide.[18] The key advantages of GC-MS include its capacity for high-resolution separation and accurate quantification of volatile PFAS. However, GC-MS is less effective for PFAS compounds with high boiling points and low vapor pressures, which are more appropriately analyzed using LC-MS. Despite this limitation, GC-MS remains an essential tool for the qualitative and quantitative assessment of volatile PFAS species.

4.1.3. Supercritical fluid chromatography. Supercritical fluid chromatography (SFC) is a promising alternative analytical technique for PFAS determination, offering rapid separation and minimal solvent consumption.[104] In this method, supercritical CO_2 serves as the mobile phase, substantially reducing the environmental impact associated with the extensive use of organic solvents in LC-MS. It is useful to separate isomeric mixtures that may co-elute in conventional liquid chromatography systems. This is because the operating temperature range is below the threshold at which enantiomers co-elute.[105] SFC-MS can also provide complementary analytical information to LC-MS such that the overall detection coverage of PFAS is enhanced. However, the high instrumental cost and the need for extensive optimization currently constrain its widespread adoption compared to LC-MS and GC-MS. Despite these challenges, SFC-MS remains a promising tool for PFAS characterization, particularly in high-throughput analytical applications.

4.1.4. Nuclear magnetic resonance. Nuclear magnetic resonance (NMR) spectroscopy is an effective tool for structural elucidation of PFAS, providing detailed molecular-level insights. In contrast to mass spectrometry, NMR does not require ionization of the analyte, and therefore, it is a non-destructive analytical technique. Among various nuclei, fluorine-19 (^{19}F-NMR) is most commonly applied for direct analysis of the fluorinated backbones of PFAS compounds.[106–108] One notable advantage of NMR is that it is able to distinguish between structural isomers and provide quantitative data on PFAS mixtures. Additionally, NMR is free from ion suppression

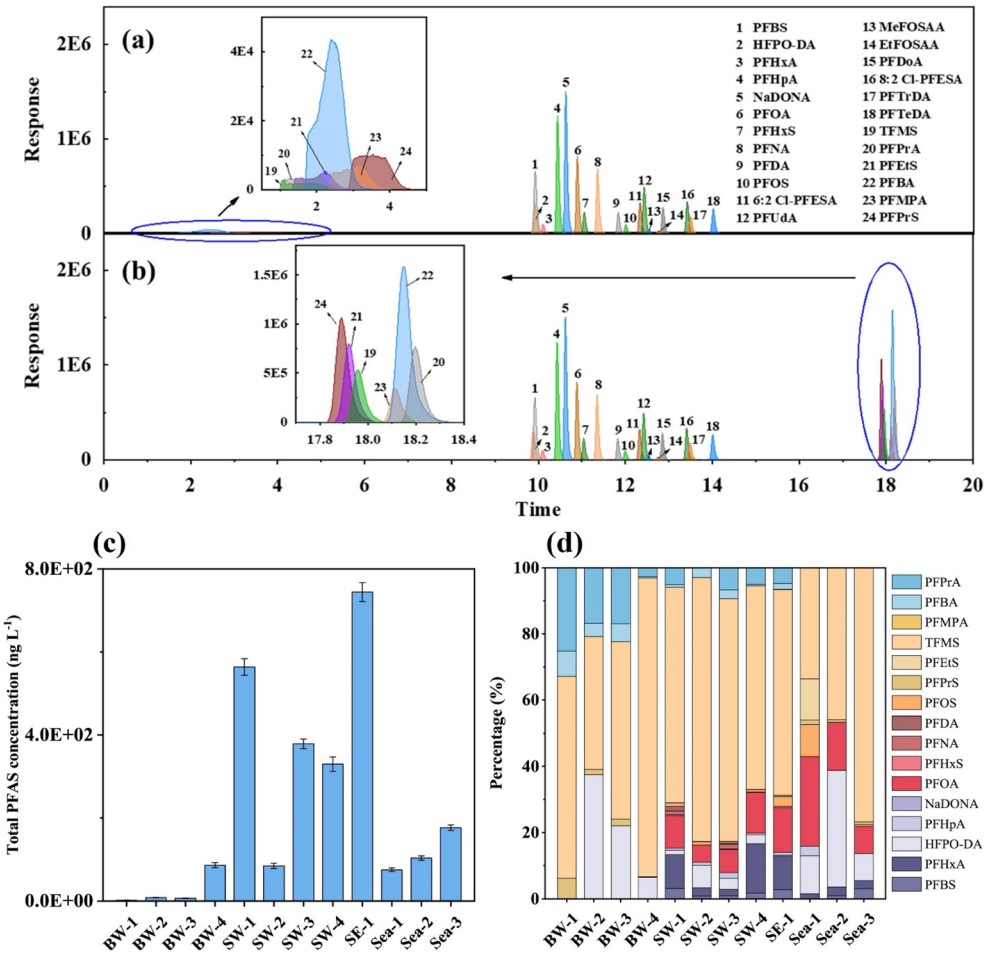

Fig. 3 PFAS analyses using conventional reverse-phase column system (a), the system combining with large volume injection (900 μL) and online solid phase extraction (b). The total concentration (c) and composition (d) of FPAS in bottled water (BW), surface water (SW), sewage effluent (SE) and seawater samples (Sea). Reprinted with the permission from ref. 98 Copyright (2024), Elsevier.

effects often affect mass spectrometry-based analyses.[109] However, NMR is less sensitive compared to LC-MS and therefore less appropriate for analysis at the trace level of PFAS. The high instrument cost and need for large-scale sample preparation also inhibit its routine usage in environmental monitoring.

4.1.5. High-resolution mass spectrometry. High-resolution mass spectrometry (HRMS) is a powerful analytical approach for identifying both known and emerging PFAS in complex environmental matrices. Techniques such as orbitrap-MS and time-of-flight HRMS enable non-targeted screening, thus enabling researchers to detect new PFAS compounds that fall outside standard reference libraries.[110,111] HRMS with ultra-high mass accuracy can effectively resolve PFAS isomers and degradation products. Also, HRMS can be used for retrospective analysis that allows previously acquired datasets to be re-examined for newly identified PFAS compounds.[112] For example, an on-line solid-phase extraction LC-HRMS method was used to determine PFAS levels in $PM_{2.5}$ (particles $\leq$ 2.5 μm in diameter) collected at urban sites in Ireland and detected perfluorobutyrate (PFBA), perfluorooctanoic acid (PFOA), perfluorooctanesulfonic acid (PFOS), and fluorotelomer sulfonates (4 : 2 FTS, 6 : 2 FTS, and 8 : 2 FTS).[113] These findings prove the effectiveness of HRMS in detecting both regulated and emerging PFAS in air samples. However, this technique requires advanced data processing equipment and skilled operators because massive databases have to be handled with great care to distill authentic signals from the ambient noise. Despite these challenges, HRMS remains an indispensable technique for environmental forensics, regulatory surveillance, and advancing PFAS research.

4.2. Advances in PFAS screening *via* AI-driven and machine learning-based detection

The integration of artificial intelligence (AI) and machine learning (ML) into physicochemical and biochemical engineering has advanced significantly over the past two decades. Machine learning algorithms, with their exceptional data-processing and predictive capabilities, have enabled rapid handling of complex datasets and facilitated high-accuracy modeling. AI-powered tools have greatly reduced the cost and time associated with experimental modeling, which is known as a traditionally resource-intensive process.[114] The accuracy and reliability of these computational models have been validated

through large-scale studies, thereby strengthening confidence in AI-based approaches for solving real-world challenges across diverse scientific and industrial domains.[115–118] In this context, AI-based detection has emerged as a promising strategy for biomedical diagnostics, environmental monitoring, and process optimization, enhancing accuracy, efficiency, and scalability in analytical science.

Identifying PFAS sources using supervised ML models has been widely applied.[119,120] For example, Kibbey *et al.*[121] used a dataset of 1197 environmental water samples containing PFAS component concentrations to train three conventional machine learning classifiers (extra trees, support-vector machines, K-neighbors) and one multilayer perceptron feedforward deep neural network. They found that all models had high classification accuracies of more than 90%. Moreover, the deep neural network and extra trees exhibited the best performance in distinguishing samples from diverse PFAS sources with accuracies of more than 95%. In a subsequent study, Kibbey *et al.*[122] continued to develop their models including random forest, gradient boosting decision trees, support vector machines, and deep neural network trained on an enlarged dataset of above 8000 samples. Using ten PFAS components as input variables, random forest algorithm was found the best classifiers with the highest accuracy of 96.4%.

AI and ML techniques have recently been applied to investigate the toxicity and immunosuppressive effects of PFAS exposure. Indeed, Xuan *et al.*[123] employed three models including random forest, extreme gradient boosting, and categorical boosting models to classify the immunosuppressive activity of 146 PFAS compounds. Among them, the random forest model demonstrated superior performance, achieving high accuracy (AUC scores of 0.96) and robustness validated through five-fold cross-validation over 500 iterations. Molecular descriptors, such as concentration and structural features, were analyzed to identify key molecular determinants driving immunosuppressive behavior.

In another study, deep transfer learning was employed to predict acute toxicity of 8163 PFAS compounds, which listed in the existing databases as illustrated in Fig. 4.[124] The experiments were conducted *via* a deep neural network trained on Mordred descriptors from a comprehensive dataset of organic compounds. This transfer learning approach successfully transferred knowledge from a large organic compound dataset to predict PFAS toxicity. Up to 3429 compounds were classified as moderately toxic according to US Environmental Protection Agency (EPA) class III. Surprisingly, for compounds with uncertain predictions, SelectiveNet was applied to improve reliability by abstaining from 40 out of 58 ambiguous cases, thereby conservatively handling high-uncertainty predictions (classified as EPA Class I). Both the experiments emphasize the importance of AI and ML in PFAS research. By efficiently processing large-scale chemical data and enhancing predictive accuracy, AI-driven models not only improve understanding of PFAS toxicity mechanisms but also support environmental risk assessments and health hazard evaluations.

Despite their promising performance, machine learning models for PFAS source identification and toxicity prediction still remain several limitations. One major concern is dataset bias. Because many training datasets are geographically or environmentally constrained, this leads to restrain the generalizability of models to unrepresented regions or sample types. In addition, validation challenges arise due to the scarcity of standardized and high-quality PFAS datasets. Thus, cross-study comparisons and model benchmarking become difficult. Variations in sampling procedures, detection limits, and analytical methods may also introduce inconsistencies that affect model accuracy and robustness. Furthermore, interpretability of predictions remains a significant issue, particularly for complex models such as deep neural networks, where the relationships between molecular descriptors and toxicological outcomes are often less transparent. This lack of transparency hinders mechanistic understanding and regulatory acceptance. Therefore, future studies should prioritize the development of explainable AI frameworks, larger and more diverse training datasets, and standardized validation protocols to enhance the reliability and interpretability of PFAS-related predictive modeling.

5. Future direction and recommendations

Although this review aims to provide critical insights into the occurrence, impacts, and detection methods for PFAS, certain specific points were not thoroughly addressed or critically analyzed. These gaps present valuable opportunities for future research and reviews on the similar topics. In the distribution sections, the occurrence of PFAS in other environments, including sediment, soil, air, and seawater, was not addressed. The omission of this detracts from the discussion of PFAS distribution across different media because these environments are considered to be large reservoirs for the storage of PFAS.[125–128] Moreover, these reservoirs can serve as intermediaries in the transport of PFAS between different environmental compartments. For instance, several reports confirmed that temperature variations at the water–air interface and sea spray aerosol processes contribute to the volatilization and atmospheric transfer of PFAS.[126,129] The impact of demographic factors on PFAS exposure was not examined in depth. Variables such as lifestyle, age, gender, race, ethnicity, religion, income, education, and health status significantly influence PFAS accumulation in humans.[130–132] Future studies should therefore integrate these demographic parameters to develop a more comprehensive and up-to-date database on PFAS exposure across populations.

The toxicological effects of PFAS on humans also require broader evaluation. Apart from the well-documented impacts on the liver, kidneys, endocrine disruption and neuron activities discussed in Section 3, PFAS exposure has adverse effects on the lungs, heart, gastrointestinal tract, and skeletal system.[133–136] Additionally, chronic exposure to PFAS may result in long-term diseases, *e.g.*, cancer and cardiovascular diseases,[137–139] as well as metabolic disorders, *e.g.*, impaired glucose metabolism and obesity.[140–143] Furthermore, the level of toxicity of PFAS is highly exposure-dependent, and can vary significantly across populations

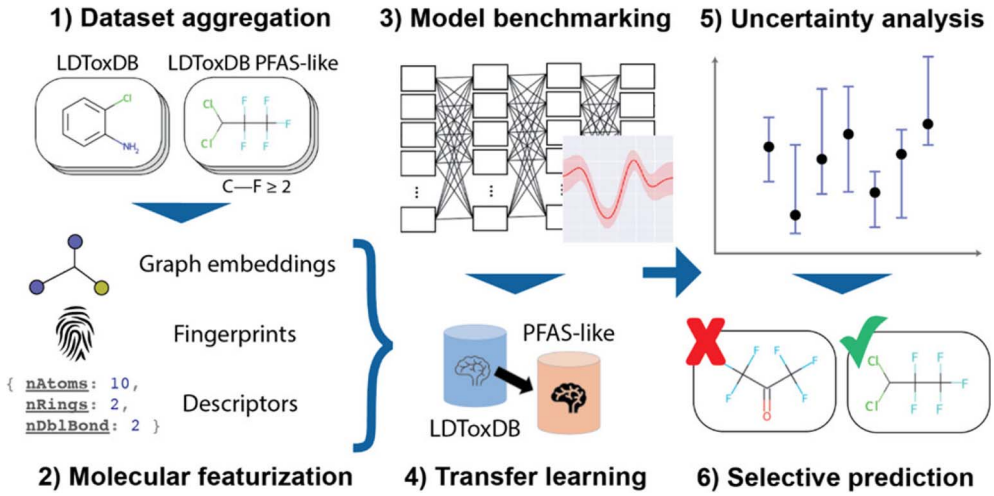

Fig. 4 Machine-learning technique for PFAS toxicity prediction. (1) Database aggregation from known toxic PFAS. (2) Molecular featurization to encode structural features. (3) Model benchmarking using different models for acute toxicity prediction. (4) Transfer learning. (5) Uncertainty analysis to reassess uncertain results for more reliable final outcomes. (6) Selective prediction using a model with higher abstention. Reprinted with the permission from ref. 124 Copyright (2021), ACS Publications.

due to geographic, occupational, and lifestyle factors.[138,144–146] Tracking PFAS concentrations in diverse demographic groups is essential for accurate health risk assessment and for informing effective regulatory measures. Oncoming studies should clarify these associations and establish evidence-based exposure limits to better safeguard public health.

Despite the significant advancements in PFAS analysis as discussed in Section 4, current analytical methods also have various challenges. The most prevalent approach is LC-MS, but this technique is prone to complex sample preparation and matrix impacts that can be detrimental to the accuracy of quantitation. Similarly, GC-MS is applicable to volatile PFAS but requires derivatization for non-volatile PFAS, leading to increased analysis time and potential errors. SFC offers faster separation and lower solvent use but struggles with highly polar compounds and demands bulky CO_2 storage systems. NMR spectroscopy is valuable for structural elucidation but is insensitive and unsuitable for trace-level detection. In the case of HRMS, it is suitable for the identification of unknown PFAS but is expensive and requires expertise in data interpretation. In further studies, researchers should leverage emerging and innovative PFAS quantification strategies, such as suspect and non-target screening with HRMS,[147–149] machine learning-assisted data analysis,[150,151] and newly developed field-deployable sensors, *e.g.*, optical-based sensor, electrochemical-based sensor,[152] molecular imprinting polymer-based nano-sensor,[153] and photothermal cantilever deflection spectroscopy with the detection limit of approximately 30 pg,[154] for real-time monitoring of PFAS. Such innovations are aimed at enhanced detection accuracy, reduced price, and broadened monitoring potential for various environmental and biological samples.

Further research should emphasize the societal, ecological, and economic consequences of PFAS contamination. For economic impacts, the U.S. Department of Defense spent over $91.6 billion in 2022 on PFAS remediation.[155] In Zhuzhou, China, treating 1 m^3 of landfill leachate would remove approximately 1 g of PFAS.[156] The U.S. Centers for Disease Control and Prevention estimated billions of dollars in medical costs incurred due to PFAS-induced diseases.[157] PFAS contamination has also caused serious agricultural losses because contaminated land and livestock are often deemed unsafe for utilization, resulting in financial hardship for farmers and food supply chain disruption.[158] Moreover, the longevity of PFAS in water sources has forced cities to invest in costly filtration systems, such as activated carbon and reverse osmosis, to render drinking water safe, adding further strain on public resources and infrastructure.[159] Because of these reasons, voluntary initiatives have been established to regulate PFAS exposure mostly in developed countries.[160] To sum up, future works should investigate these aspects more to make a broader and more critical review of PFAS effects.

Author contributions

Linh Q. Phan: conceptualization, investigation, writing – original draft. Kien G. Nguyen: validation, data curation, formal analysis. Thuan V. Tran: writing – original draft, writing – review & editing, supervision, project administration. All authors read and approved the final manuscript.

Conflicts of interest

The authors declare that there are no conflicts of interest.

Data availability

No primary research results, software or code have been included and no new data were generated or analysed as part of this review.

Supplementary information (SI) is available. See DOI: https://doi.org/10.1039/d5ra05298j.

Acknowledgements

We acknowledge Nguyen Tat Thanh University, Ho Chi Minh City, Vietnam for supporting this study.

References

1 G. V. Koulini, V. Vinayagam, I. M. Nambi and R. R. Krishna, *J. Water Process Eng.*, 2024, **66**, 105988.
2 K. Sivagami, P. Sharma, A. V. Karim, G. Mohanakrishna, S. Karthika, G. Divyapriya, R. Saravanathamizhan and A. N. Kumar, *Sci. Total Environ.*, 2023, **861**, 160440.
3 E. F. Houtz and D. L. Sedlak, *Environ. Sci. Technol.*, 2012, **46**, 9342–9349.
4 M. G. Evich, M. J. B. Davis, J. P. McCord, B. Acrey, J. A. Awkerman, D. R. U. Knappe, A. B. Lindstrom, T. F. Speth, C. Tebes-Stevens, M. J. Strynar, Z. Wang, E. J. Weber, W. M. Henderson and J. W. Washington, *Science*, 2022, **375**, eabg9065.
5 J. Zheng, S. Liu, J. Yang, S. Zheng and B. Sun, *Sci. Total Environ.*, 2024, **953**, 176158.
6 J. L. Domingo, *Environ. Res.*, 2025, **272**, 121181.
7 L. Jane L Espartero, M. Yamada, J. Ford, G. Owens, T. Prow and A. Juhasz, *Environ. Res.*, 2022, **212**, 113431.
8 I. T. Cousins, J. H. Johansson, M. E. Salter, B. Sha and M. Scheringer, *Environ. Sci. Technol.*, 2022, **56**, 11172–11179.
9 N. Donley, C. Cox, K. Bennett, A. M. Temkin, D. Q. Andrews and O. V. Naidenko, *Environ. Health Perspect.*, 2024, **132**, 075003.
10 A. U. Rehman, M. Crimi and S. Andreescu, *Trends Environ. Anal. Chem.*, 2023, **37**, e00198.
11 A. Amziane, F. Monteau, A. el djalil Lalaouna, B. Alamir, B. Le Bizec and G. Dervilly, *J. Chromatogr. B*, 2022, **1210**, 123455.
12 Y. Wang, M. Liu, S. Vo Duy, G. Munoz, S. Sauvé and J. Liu, *Sci. Total Environ.*, 2024, **943**, 173682.
13 Y. Cui, S. Wang, D. Han and H. Yan, *TrAC, Trends Anal. Chem.*, 2024, **176**, 117754.
14 T. Zhou, X. Li, H. Liu, S. Dong, Z. Zhang, Z. Wang, J. Li, L. D. Nghiem, S. J. Khan and Q. Wang, *J. Hazard. Mater.*, 2024, **466**, 133637.
15 C. Venkatesh Reddy, R. Kumar, P. Chakrabortty, B. Karmakar, S. Pottipati, A. Kundu and B.-H. Jeon, *Chem. Eng. J.*, 2024, **492**, 152272.
16 T. H. Bui, N. Zuverza-Mena, C. O. Dimkpa, S. L. Nason, S. Thomas and J. C. White, *Environ. Pollut.*, 2024, **344**, 123335.
17 M. A. G. Wallace, M. G. Smeltz, J. M. Mattila, H. K. Liberatore, S. R. Jackson, E. P. Shields, X. Xhani, E. Y. Li and J. H. Johansson, *Chemosphere*, 2024, **358**, 142129.
18 Y. Shen, L. Wang, Y. Ding, S. Liu, Y. Li, Z. Zhou and Y. Liang, *Crit. Rev. Anal. Chem.*, 2024, **54**, 3171–3195.
19 I. Rosato, T. Bonato, T. Fletcher, E. Batzella and C. Canova, *Environ. Res.*, 2024, **242**, 117743.
20 L. Ricolfi, C. Vendl, J. Bräunig, M. D. Taylor, D. Hesselson, G. Gregory Neely, M. Lagisz and S. Nakagawa, *Environ. Int.*, 2024, **190**, 108860.
21 J. Fang, S. Li, T. Gu, A. Liu, R. Qiu and W. Zhang, *J. Environ. Chem. Eng.*, 2024, **12**, 111833.
22 M. Vakili, G. Cagnetta, S. Deng, W. Wang, Z. Gholami, F. Gholami, W. Dastyar, A. Mojiri and L. Blaney, *J. Hazard. Mater.*, 2024, **471**, 134429.
23 G. Feng, B. Zhou, R. Yuan, S. Luo, N. Gai and H. Chen, *Sci. Total Environ.*, 2024, **925**, 171785.
24 Z. Liu, M. Liao, L. Wang and S. Zhuang, *Rev. Environ. Sci. Bio/Technol.*, 2025, **24**, 63–95.
25 C. Gomri, B. T. Benkhaled, M. Cretin and M. Semsarilar, *Macromol. Chem. Phys.*, 2024, **225**, 2400012.
26 F. Liu, J. J. Pignatello, R. Sun, X. Guan and F. Xiao, *ACS ES&T Water*, 2024, **4**, 1191–1205.
27 A. Behnami, M. Pourakbar, A. S.-R. Ayyar, J.-W. Lee, G. Gagnon and K. Zoroufchi Benis, *Chemosphere*, 2024, **357**, 142088.
28 F. Calore, E. Badetti, A. Bonetto, A. Pozzobon and A. Marcomini, *Emerging Contam.*, 2024, **10**, 100303.
29 D. Liang, C. Li, H. Chen, E. Sørmo, G. Cornelissen, Y. Gao, F. Reguyal, A. Sarmah, J. Ippolito, C. Kammann, F. Li, Y. Sailaukhanuly, H. Cai, Y. Hu, M. Wang, X. Li, X. Cui, B. Robinson, E. Khan, J. Rinklebe, T. Ye, F. Wu, X. Zhang and H. Wang, *Sci. Total Environ.*, 2024, **951**, 174962.
30 P. Ramos and D. J. Ashworth, *Sci. Total Environ.*, 2024, **927**, 172275.
31 P. B. McMahon, A. K. Tokranov, L. M. Bexfield, B. D. Lindsey, T. D. Johnson, M. A. Lombard and E. Watson, *Environ. Sci. Technol.*, 2022, **56**, 2279–2288.
32 D. Song, B. Qiao, Y. Yao, L. Zhao, X. Wang, H. Chen, L. Zhu and H. Sun, *J. Hazard. Mater.*, 2023, **460**, 132411.
33 C. Sáez, A. Bautista, O. Nikolenko, L. Scheiber, M. Llorca, A. Jurado, M. Farré and E. Pujades-Garnes, *Environ. Pollut.*, 2024, **358**, 124468.
34 A. Ramírez-Canon, A. Paola Becerra-Quiroz and F. Herrera-Jacquelin, *Environ. Adv.*, 2022, **8**, 100223.
35 Z. Huang, X. Zhang, X. Wang, Z. Deji and H. K. Lee, *J. Agric. Food Chem.*, 2022, **70**, 10836–10846.
36 R. Lasters, T. Groffen, M. Eens, D. Coertjens, W. A. Gebbink, J. Hofman and L. Bervoets, *Chemosphere*, 2022, **308**, 136283.
37 P. Vázquez Loureiro, K.-H. Nguyen, A. Rodríguez Bernaldo de Quirós, R. Sendón, K. Granby and A. A. Niklas, *Chemosphere*, 2024, **360**, 142360.
38 A. A. Schultz, N. Stanton, B. Shelton, R. Pomazal, M. A. Lange, R. Irving, J. Meiman and K. C. Malecki, *J. Exposure Sci. Environ. Epidemiol.*, 2023, **33**, 766–777.
39 M. Suzuki, S. Nilsson, C. E. Shepherd, I. Zammit, E. Suryana, N. Mueller, G. Halliday, X. Wang, C. Symeonides, S. Dunlop and J. F. Mueller, *Environ. Sci. Technol.*, 2025, **59**, 3366–3375.
40 Y. Lu, R. Guan, N. Zhu, J. Hao, H. Peng, A. He, C. Zhao, Y. Wang and G. Jiang, *Crit. Rev. Environ. Sci. Technol.*, 2024, **54**, 95–116.
41 Y. Cao and C. Ng, *Environ. Sci.:Processes Impacts*, 2021, **23**, 1623–1640.
42 W. Hu, M.-Y. Zhang, L.-Y. Liu, Z.-F. Zhang and Y. Guo, *J. Hazard. Mater.*, 2023, **442**, 130003.

43 G. Zheng, E. Schreder, J. C. Dempsey, N. Uding, V. Chu, G. Andres, S. Sathyanarayana and A. Salamova, *Environ. Sci. Technol.*, 2021, **55**, 7510–7520.
44 A. J. Blomberg, E. Norén, L. S. Haug, C. Lindh, A. Sabaredzovic, D. Pineda, K. Jakobsson and C. Nielsen, *Environ. Health Perspect.*, 2023, **131**, 017005.
45 L. Fábelová, A. Beneito, M. Casas, A. Colles, L. Dalsager, E. Den Hond, C. Dereumeaux, K. Ferguson, L. Gilles, E. Govarts, A. Irizar, M. J. Lopez Espinosa, P. Montazeri, B. Morrens, H. Patayová, K. Rausová, D. Richterová, L. Rodriguez Martin, L. Santa-Marina, T. Schettgen, G. Schoeters, L. S. Haug, M. Uhl, G. D. Villanger, M. Vrijheid, C. Zaros and Ľ. Palkovičová Murínová, *Chemosphere*, 2023, **313**, 137530.
46 X. Huo, W. Liang, W. Tang, Y. Ao, Y. Tian, Q. Zhang and J. Zhang, *Chemosphere*, 2023, **332**, 138863.
47 H. E. Hampson, E. Costello, D. I. Walker, H. Wang, B. O. Baumert, D. Valvi, S. Rock, D. P. Jones, M. I. Goran, F. D. Gilliland, D. V. Conti, T. L. Alderete, Z. Chen, L. Chatzi and J. A. Goodrich, *Environ. Int.*, 2024, **185**, 108454.
48 H. Sultan, J. P. Buckley, H. J. Kalkwarf, K. M. Cecil, A. Chen, B. P. Lanphear, K. Yolton and J. M. Braun, *Environ. Res.*, 2023, **231**, 115953.
49 R. Vestergren, F. Orata, U. Berger and I. T. Cousins, *Environ. Sci. Pollut. Res.*, 2013, **20**, 7959–7969.
50 R. Zhou, J. Peng, L. Zhang, Y. Sun, J. Yan and H. Jiang, *Food Funct.*, 2024, **15**, 7375–7386.
51 K. Lucas, L. G. T. Gaines, T. Paris-Davila and L. A. Nylander-French, *Am. J. Ind. Med.*, 2023, **66**, 379–392.
52 B. I. Freberg, L. S. Haug, R. Olsen, H. L. Daae, M. Hersson, C. Thomsen, S. Thorud, G. Becher, P. Molander and D. G. Ellingsen, *Environ. Sci. Technol.*, 2010, **44**, 7723–7728.
53 P. E. Rosenfeld, K. R. Spaeth, L. L. Remy, V. Byers, S. A. Muerth, R. C. Hallman, J. Summers-Evans and S. Barker, *Environ. Res.*, 2023, **220**, 115164.
54 N.-U.-S. Mazumder, M. T. Hossain, F. T. Jahura, A. Girase, A. S. Hall, J. Lu and R. B. Ormond, *Front. Mater.*, 2023, **10**, 1143411.
55 C. L. Mitchell, J. Hollister, J. M. Fisher, S. C. Beitel, F. Ramadan, S. O'Leary, Z. T. Fan, K. Lutrick, J. L. Burgess and K. D. Ellingson, *J. Exposure Sci. Environ. Epidemiol.*, 2025, **35**, 437–444.
56 J. Trowbridge, R. R. Gerona, T. Lin, R. A. Rudel, V. Bessonneau, H. Buren and R. Morello-Frosch, *Environ. Sci. Technol.*, 2020, **54**, 3363–3374.
57 K. Y. Christensen, B. A. Thompson, M. Werner, K. Malecki, P. Imm and H. A. Anderson, *Int. J. Hyg. Environ. Health*, 2016, **219**, 184–194.
58 W. A. Wattigney, E. Irvin-Barnwell, Z. Li, S. I. Davis, S. Manente, J. Maqsood, D. Scher, R. Messing, N. Schuldt, S.-A. Hwang, K. M. Aldous, E. L. Lewis-Michl and A. Ragin-Wilson, *Int. J. Hyg. Environ. Health*, 2019, **222**, 125–135.
59 A. Yamada, N. Bemrah, B. Veyrand, C. Pollono, M. Merlo, V. Desvignes, V. Sirot, P. Marchand, A. Berrebi, R. Cariou, J. P. Antignac, B. Le Bizec and J. C. Leblanc, *Sci. Total Environ.*, 2014, **491–492**, 170–175.
60 W. Nassazzi, T.-C. Wu, J. Jass, F. Y. Lai and L. Ahrens, *Environ. Pollut.*, 2023, **333**, 122038.
61 S. Brendel, É. Fetter, C. Staude, L. Vierke and A. Biegel-Engler, *Environ. Sci. Eur.*, 2018, **30**, 9.
62 T. Jiang, W. Zhang and Y. Liang, *Sci. Total Environ.*, 2022, **838**, 156640.
63 H. Liu, W. Hu, X. Li, F. Hu, Y. Liu, T. Xie, B. Liu, Y. Xi, Z. Su and C. Zhang, *Chemosphere*, 2022, **289**, 133137.
64 K. D. Rock, M. E. Polera, T. C. Guillette, H. M. Starnes, K. Dean, M. Watters, D. Stevens-Stewart and S. M. Belcher, *Environ. Sci. Technol.*, 2023, **57**, 9567–9579.
65 C. C. Witt, C. R. Gadek, J.-L. E. Cartron, M. J. Andersen, M. L. Campbell, M. Castro-Farías, E. F. Gyllenhaal, A. B. Johnson, J. L. Malaney, K. N. Montoya, A. Patterson, N. T. Vinciguerra, J. L. Williamson, J. A. Cook and J. L. Dunnum, *Environ. Res.*, 2024, **249**, 118229.
66 D. Herzke, V. Nikiforov, L. W. Y. Yeung, B. Moe, H. Routti, T. Nygård, G. W. Gabrielsen and L. Hanssen, *Environ. Int.*, 2023, **171**, 107640.
67 A. J. Levine, E. Z. Bean, F. O. Hinz, P. C. Wilson and A. J. Reisinger, *J. Environ. Manage.*, 2023, **343**, 118185.
68 Q. Gu, Y. Wen, H. Wu and X. Cui, *Sci. Total Environ.*, 2023, **862**, 160684.
69 Q. Jin, Y. Zhang, Y. Gu, Y. Shi and Y. Cai, *J. Environ. Sci.*, 2025, **154**, 378–389.
70 S. Felizeter, M. S. McLachlan and P. de Voogt, *Environ. Sci. Technol.*, 2012, **46**, 11735–11743.
71 H. Zhao, B. Qu, Y. Guan, J. Jiang and X. Chen, *Springerplus*, 2016, **5**, 541.
72 Z. Niu, Z. Duan, W. He, T. Chen, H. Tang, S. Du, J. Sun, H. Chen, Y. Hu, Y. Iijima, S. Han, J. Li and Z. Zhao, *J. Hazard. Mater.*, 2024, **471**, 134312.
73 M. E. Solan, C. P. Koperski, S. Senthilkumar and R. Lavado, *Environ. Res.*, 2023, **223**, 115424.
74 C. E. Enyoh, P. E. Ovuoraye, W. Qingyue and W. Wang, *J. Hazard. Mater.*, 2023, **459**, 132103.
75 Z. Pan, Y. Guo, Q. Zhou, Q. Wang, S. Pan, S. Xu and L. Li, *Environ. Sci. Pollut. Res.*, 2023, **30**, 52535–52548.
76 B. Rudzanova, J. Vlaanderen, J. Kalina, P. Piler, M. Zvonar, J. Klanova, L. Blaha and O. Adamovsky, *Environ. Res.*, 2023, **229**, 115969.
77 G. C. Addicks, A. Rowan-Carroll, K. Leingartner, A. Williams, M. J. Meier, L. Lorusso, C. L. Yauk and E. Atlas, *Toxicol. Sci.*, 2025, **207**, 161–180.
78 S. E. Fenton, A. Ducatman, A. Boobis, J. C. DeWitt, C. Lau, C. Ng, J. S. Smith and S. M. Roberts, *Environ. Toxicol. Chem.*, 2020, **40**, 606–630.
79 L. Kashobwe, F. Sadrabadi, A. Braeuning, P. E. G. Leonards, T. Buhrke and T. Hamers, *Arch. Toxicol.*, 2024, **98**, 3381–3395.
80 W. Murase, A. Kubota, A. Ikeda-Araki, M. Terasaki, K. Nakagawa, R. Shizu, K. Yoshinari and H. Kojima, *Toxicology*, 2023, **494**, 153577.
81 J. Qiu, X. Huo, Y. Dai, Y. Huang and X. Xu, *Ecotoxicol. Environ. Saf.*, 2025, **302**, 118757.

82 K. M. Ríos-Bonilla, D. S. Aga, J. Lee, M. König, W. Qin, J. R. Cristobal, G. E. Atilla-Gokcumen and B. I. Escher, *Environ. Sci. Technol.*, 2024, **58**, 16774–16784.
83 G. A. Franco, F. Molinari, Y. Marino, N. Tranchida, F. Inferrera, R. Fusco, R. Di Paola, R. Crupi, S. Cuzzocrea, E. Gugliandolo and D. Britti, *Environ. Toxicol. Pharmacol.*, 2024, **109**, 104496.
84 M. J. Marchese, T. Zhu, A. B. Hawkey, K. Wang, E. Yuan, J. Wen, S. E. Be, E. D. Levin and L. Feng, *Sci. Total Environ.*, 2024, **917**, 170459.
85 Y. He, C. Hu, Y. Zhang, X. Fan, W. Gao, J. Fang, Y. Wang, Y. Xu and L. Jin, *Environ. Pollut.*, 2023, **329**, 121707.
86 W. Zhang, N. Sheng, M. Wang, H. Zhang and J. Dai, *Aquat. Toxicol.*, 2016, **175**, 269–276.
87 M. Averina, S. Huber, B. Almås, J. Brox, B. K. Jacobsen, A.-S. Furberg and G. Grimnes, *Environ. Res.*, 2024, **242**, 117703.
88 W. Zhan, W. Qiu, Y. Ao, W. Zhou, Y. Sun, H. Zhao and J. Zhang, *Environ. Health Perspect.*, 2023, **131**, 057001.
89 E. Haverinen, M. F. Fernandez, V. Mustieles and H. Tolonen, *Int. J. Environ. Res. Public Health*, 2021, **18**, 13047.
90 C.-H. Li, X.-M. Ren and L.-H. Guo, *Environ. Sci. Technol.*, 2019, **53**, 3287–3295.
91 L. Groisman, T. Berman, A. Quinn, G. Pariente, E. Rorman, I. Karakis, R. Gat, B. Sarov and L. Novack, *Ecotoxicol. Environ. Saf.*, 2023, **262**, 115165.
92 K. Pan, J. Xu, X. Long, L. Yang, Z. Huang and J. Yu, *Environ. Res.*, 2023, **232**, 116362.
93 Y. Du, Z. Cai, G. Zhou, W. Liang, Q. Man and W. Wang, *Ecotoxicol. Environ. Saf.*, 2022, **236**, 113508.
94 X. Zhang, X. Ren, W. Sun, N. Griffin, L. Wang and H. Liu, *Toxicology*, 2023, **493**, 153551.
95 X. Fang, G. Gao, H. Xue, X. Zhang and H. Wang, *Toxicology*, 2012, **294**, 109–115.
96 Y. Zhang, V. Mustieles, Q. Sun, B. Coull, T. McElrath, S. L. Rifas-Shiman, L. Martin, Y. Sun, Y.-X. Wang, E. Oken, A. Cardenas and C. Messerlian, *JAMA Netw. Open*, 2023, **6**, e2314934.
97 J. Shen, Y. Mao, H. Zhang, H. Lou, L. Zhang, J. P. Moreira and F. Jin, *Environ. Pollut.*, 2024, **359**, 124474.
98 J. Zou, M. Zhao, S.-A. Chan, Y. Song, S. Yan and W. Song, *J. Chromatogr. A*, 2024, **1734**, 465324.
99 J. de O. Mozzaquatro, I. A. César, A. E. B. Pinheiro and E. D. Caldas, *Food Chem.*, 2022, **375**, 131643.
100 S. Taniyasu, K. Kannan, L. W. Y. Yeung, K. Y. Kwok, P. K. S. Lam and N. Yamashita, *Anal. Chim. Acta*, 2008, **619**, 221–230.
101 M. T.-A. Hassan, X. Chen, P. I. J. Fnu, F. J. Osonga, O. A. Sadik, M. Li and H. Chen, *J. Hazard. Mater.*, 2024, **465**, 133366.
102 P. Vera, E. Canellas, N. Dreolin, J. Goshawk and C. Nerín, *Talanta*, 2024, **266**, 124999.
103 S. Valsecchi, M. Rusconi and S. Polesello, *Anal. Bioanal. Chem.*, 2013, **405**, 143–157.
104 L. Si-Hung and T. Bamba, *TrAC, Trends Anal. Chem.*, 2022, **149**, 116550.
105 W. Ren-Qi, O. Teng-Teng, N. Siu-Choon and T. Weihua, *TrAC, Trends Anal. Chem.*, 2012, **37**, 83–100.
106 J. R. Gauthier and S. A. Mabury, *Anal. Chem.*, 2022, **94**, 3278–3286.
107 M. Thijs, E. Laletas, C. M. Quinn, S. V. Raguraman, B. Carr and P. Bierganns, *Anal. Chem.*, 2024, **96**, 8282–8290.
108 D. Camdzic, R. A. Dickman, A. S. Joyce, J. S. Wallace, P. L. Ferguson and D. S. Aga, *Anal. Chem.*, 2023, **95**, 5484–5488.
109 A. J. Taylor, A. Dexter and J. Bunch, *Anal. Chem.*, 2018, **90**, 5637–5645.
110 N. Wiedmaier-Czerny and W. Vetter, *Anal. Bioanal. Chem.*, 2023, **415**, 875–885.
111 D. Zacs, J. Rjabova, I. Pugajeva, I. Nakurte, A. Viksna and V. Bartkevics, *J. Chromatogr. A*, 2014, **1366**, 73–83.
112 A. Kaufmann, A. Arrizabalaga-Larrañaga, M. H. Blokland and S. S. Sterk, *Food Control*, 2023, **147**, 109611.
113 I. Kourtchev, S. Hellebust, E. Heffernan, J. Wenger, S. Towers, E. Diapouli and K. Eleftheriadis, *Sci. Total Environ.*, 2022, **835**, 155496.
114 C. Yaiprasert and A. N. Hidayanto, *Int. J. Inf. Manage. Data Insights*, 2024, **4**, 100209.
115 R. Gupta, S. Kumari, A. Senapati, R. K. Ambasta and P. Kumar, *Ageing Res. Rev.*, 2023, **90**, 102013.
116 A. Konya and P. Nematzadeh, *Sci. Total Environ.*, 2024, **906**, 167705.
117 C. van Dun, L. Moder, W. Kratsch and M. Röglinger, *Decis. Support Syst.*, 2023, **165**, 113880.
118 P. P. Mondal, A. Galodha, V. K. Verma, V. Singh, P. L. Show, M. K. Awasthi, B. Lall, S. Anees, K. Pollmann and R. Jain, *Bioresour. Technol.*, 2023, **370**, 128523.
119 S. Yaghoobian, M. A. Ramirez-Ubillus, L. Zhai and J.-H. Hwang, *Chem. Sci.*, 2025, **16**, 13564–13573.
120 J. Park, J.-H. Baik, S. Adjei-Nimoh and W. H. Lee, *Sci. Total Environ.*, 2025, **980**, 179536.
121 T. C. G. Kibbey, R. Jabrzemski and D. M. O'Carroll, *Chemosphere*, 2020, **252**, 126593.
122 T. C. G. Kibbey, R. Jabrzemski and D. M. O'Carroll, *Chemosphere*, 2021, **275**, 130124.
123 Y. Xuan, Y. Wang, R. Li, Y. Zhong, N. Wang, L. Zhang, Q. Chen, S. Yu and J. Yuan, *Toxicol. Mech. Methods*, 2025, **35**, 72–80.
124 J. Feinstein, G. Sivaraman, K. Picel, B. Peters, Á. Vázquez-Mayagoitia, A. Ramanathan, M. MacDonell, I. Foster and E. Yan, *J. Chem. Inf. Model.*, 2021, **61**, 5793–5803.
125 M. E. Morales-McDevitt, J. Becanova, A. Blum, T. A. Bruton, S. Vojta, M. Woodward and R. Lohmann, *Environ. Sci. Technol. Lett.*, 2021, **8**, 897–902.
126 J. Garnett, C. Halsall, M. Thomas, O. Crabeck, J. France, H. Joerss, R. Ebinghaus, J. Kaiser, A. Leeson and P. M. Wynn, *Environ. Sci. Technol.*, 2021, **55**, 9601–9608.
127 J. Reinikainen, N. Perkola, L. Äystö and J. Sorvari, *Sci. Total Environ.*, 2022, **829**, 154237.
128 X. Jiang, Z. Zhou, Z. Qin, T. Ou, Q. Zhang, H. Zhang, X. Wu, S. He, B. Meng, Y. Ge, J. Huang, Y. Zhang, Z. Peng, G. Yu and S. Deng, *Environ. Sci. Technol.*, 2024, **58**, 22744–22754.

129 B. Sha, J. H. Johansson, P. Tunved, P. Bohlin-Nizzetto, I. T. Cousins and M. E. Salter, *Environ. Sci. Technol.*, 2022, **56**, 228–238.
130 N. M. DeLuca, K. Thomas, A. Mullikin, R. Slover, L. W. Stanek, A. N. Pilant and E. A. Cohen Hubal, *J. Exposure Sci. Environ. Epidemiol.*, 2023, **33**, 710–724.
131 M. M. Borghese, A. Ward, S. MacPherson, K. E. Manz, E. Atlas, M. Fisher, T. E. Arbuckle, J. M. Braun, M. F. Bouchard and J. Ashley-Martin, *Environ. Health*, 2024, **23**, 55.
132 J. A. Kemper, E. Sharp, S. Yi, E. M. Leitao, L. P. Padhye, M. Kah, J. L.-Y. Chen and K. Gobindlal, *J. Cleaner Prod.*, 2024, **442**, 140866.
133 A. Koskela, J. Koponen, P. Lehenkari, M. Viluksela, M. Korkalainen and J. Tuukkanen, *Sci. Rep.*, 2017, **7**, 6841.
134 Y. Xu, Y. Li, K. Scott, C. H. Lindh, K. Jakobsson, T. Fletcher, B. Ohlsson and E. M. Andersson, *Environ. Res.*, 2020, **181**, 108923.
135 Z.-J. Wen, Y.-J. Wei, Y.-F. Zhang and Y.-F. Zhang, *Arch. Toxicol.*, 2023, **97**, 1195–1245.
136 J. Dragon, M. Hoaglund, A. R. Badireddy, G. Nielsen, J. Schlezinger and A. Shukla, *Int. J. Mol. Sci.*, 2023, **24**, 8539.
137 L. Dunder, S. Salihovic, P. M. Lind, S. Elmståhl and L. Lind, *Environ. Int.*, 2023, **177**, 107979.
138 A. Biggeri, G. Stoppa, L. Facciolo, G. Fin, S. Mancini, V. Manno, G. Minelli, F. Zamagni, M. Zamboni, D. Catelan and L. Bucchi, *Environ. Health*, 2024, **23**, 42.
139 J. Yang, K. Zhang, C. Shen, P. Tang, S. Tu, J. Li, L. Chen and W. Yang, *Int. Heart J.*, 2023, **64**, 23–036.
140 G. Yu, M. Jin, Y. Huang, R. Aimuzi, T. Zheng, M. Nian, Y. Tian, W. Wang, Z. Luo, L. Shen, X. Wang, Q. Du, W. Xu and J. Zhang, *Environ. Int.*, 2021, **156**, 106621.
141 Z. Chen, T. Yang, D. I. Walker, D. C. Thomas, C. Qiu, L. Chatzi, T. L. Alderete, J. S. Kim, D. V. Conti, C. V. Breton, D. Liang, E. R. Hauser, D. P. Jones and F. D. Gilliland, *Environ. Int.*, 2020, **145**, 106091.
142 Y. Ren, L. Jin, F. Yang, H. Liang, Z. Zhang, J. Du, X. Song, M. Miao and W. Yuan, *Environ. Health*, 2020, **19**, 88.
143 N. Ding, C. A. Karvonen-Gutierrez, W. H. Herman, A. M. Calafat, B. Mukherjee and S. K. Park, *Int. J. Hyg. Environ. Health*, 2021, **235**, 113777.
144 C. C. Bach, Z. Liew, N. B. Matthiesen, T. B. Henriksen, B. H. Bech, E. A. Nøhr, E. C. Bonefeld-Jørgensen and J. Olsen, *Environ. Res.*, 2022, **212**, 113262.
145 C. H. Yu, C. D. Riker, S. Lu and Z. (Tina) Fan, *Int. J. Hyg. Environ. Health*, 2020, **223**, 34–44.
146 N. Ding, S. D. Harlow, S. Batterman, B. Mukherjee and S. K. Park, *Environ. Int.*, 2020, **135**, 105381.
147 S. Chu and R. J. Letcher, *J. Chromatogr. A*, 2024, **1715**, 464584.
148 L.-A. Koronaiou, C. Nannou, N. Xanthopoulou, G. Seretoudi, D. Bikiaris and D. A. Lambropoulou, *Microchem. J.*, 2022, **179**, 107457.
149 K. Anagnostopoulpou, C. Nannou, V. G. Aschonitis and D. A. Lambropoulou, *Sci. Total Environ.*, 2022, **849**, 157887.
150 Y. Fan, Y. Deng, Y. Yang, X. Deng, Q. Li, B. Xu, J. Pan, S. Liu, Y. Kong and C.-E. Chen, *Environ. Sci.:Adv.*, 2024, **3**, 198–207.
151 J. Zhang, K. Fu, S. Zhong and J. Luo, *Environ. Sci. Technol.*, 2025, **59**, 3603–3612.
152 D. Thompson, N. Zolfigol, Z. Xia and Y. Lei, *Sens. Acutators Rep.*, 2024, **7**, 100189.
153 B. Qian, J. L. Rayner, G. B. Davis, A. Trinchi, G. Collis, I. (Louis) Kyratzis and A. Kumar, *Ecotoxicol. Environ. Saf.*, 2024, **284**, 116932.
154 Y. Zhao, N. K. Jannabhatla and T. Thundat, *ECS Sens. Plus*, 2025, **4**, 013401.
155 D. Klingelhöfer, M. Braun, D. A. Groneberg and D. Brüggmann, *Chemosphere*, 2024, **354**, 141694.
156 D. Feng, C. Song and W. Mo, *J. Environ. Manage.*, 2021, **289**, 112558.
157 V. Obsekov, L. G. Kahn and L. Trasande, *Exposure Health*, 2023, **15**, 373–394.
158 S. P. J. van Leeuwen, A. M. Verschoor, H. J. van der Fels-Klerx, M. G. M. van de Schans and B. J. A. Berendsen, *npj Sci. Food*, 2024, **8**, 34.
159 V. Franke, P. McCleaf, K. Lindegren and L. Ahrens, *Environ. Sci.:Water Res. Technol.*, 2019, **5**, 1836–1843.
160 Z. Wang, J. C. DeWitt, C. P. Higgins and I. T. Cousins, *Environ. Sci. Technol.*, 2017, **51**, 2508–2518.